

Experimental and theoretical study of metallic iodine*

A. K. McMahan, B. L. Hord, and M. Ross

Lawrence Livermore Laboratory, University of California, Livermore, California 94550

(Received 12 July 1976)

Insulating molecular iodine is known to transform gradually to a metallic state between 4 and 17 GPa of pressure at room temperature. An anomaly found in early shock-compression experiments has been taken to indicate that actual dissociation of the iodine molecules does not occur until much higher pressures. We report new experimental and theoretical results for the shock-compression curve that show no evidence for this anomaly. Furthermore, our calculations for an assumed monatomic, metallic phase are in agreement with the new shock data, and suggest that the I_2 bond may be destroyed in the vicinity of the metallic transition.

I. INTRODUCTION

Solid iodine is one of a small number of elemental materials whose pressure-induced metallization can be studied under conditions readily accessible in the laboratory. It is normally a diatomic molecular insulator and achieves metallic conductivity under relatively low pressures. At room temperature and 1 atm of pressure, iodine is a base-centered orthorhombic crystal with the I_2 molecular axes lying in the ac plane. Electrical resistivity¹⁻⁵ measurements indicate a gradual onset of metallic conductivity as iodine is compressed. The resistivity of the insulating phase begins to drop at 4 GPa (40 kbar) and reaches its metallic limiting value at about 13.5 GPa perpendicular to the ac plane (parallel at about 17 GPa).⁶ There is no evidence of discontinuous behavior in the resistivity measurements that might suggest a first-order phase transition. Independent measurements of the optical gap are consistent with these results.^{3,7} Although evidence from x-ray powder-diffraction experiments indicates the possible presence of structural changes above 4 GPa, no definitive conclusions can be drawn.⁸ Pressure-volume isotherms have been obtained both from x-ray^{8,9} and piston-displacement^{10,11} experiments. There is wide disagreement amongst these results, but generally there is no evidence of anomalous behavior that might be correlated with the resistivity phenomena.

The most extensive measurements of iodine from 15 to 110 GPa are from shock-compression experiments. Alder and Christian¹² reported an abrupt change in the slope of the shock-compression curve at 70 GPa and a relative compression of $V/V_0 = 0.53$, an apparent first-order phase transition, which they inferred as the diatomic molecular to monatomic metallic transition in iodine. In standard fashion they estimated the temperature increase resulting from shock heating and predicted the transition pressure at 300 K to be about 30

GPa. It should be noted that the shock work of Alder and Christian preceded the static resistivity measurements so that their conclusions were drawn without the knowledge that iodine already attained metallic conductivities at lower pressures. A monatomic iodine lattice would, of course, be metallic, since the $5p$ band would only be $\frac{5}{6}$ full. However, if the molecules do not dissociate until 30 GPa as Alder and Christian suggest, then the onset of metallic conductivity at lower pressures must be a result of the overlap of the full valence band with the empty conduction band in a still molecular phase.

Since neither the shock nor static experiments provide sufficient information to assign a monatomic or molecular structure to the high-pressure phases, we have at least two possibilities with which to interpret the decrease in electrical resistivity and the anomalous shock behavior. One possibility is that the molecular-iodine conduction bands begin to overlap the insulating valence bands at 4 GPa, decreasing the resistivity as observed statically; and at 30 GPa (300 K) or 70 GPa (1 eV), the molecular bonds are broken to form monatomic metallic iodine as observed dynamically. In a second scenario iodine undergoes a transition from a molecular insulating structure to a monatomiclike metal over the range of 4–17 GPa. The dynamic transition at high pressure must then be ascribed to either melting, electronic effects, or some other phenomena.

In this paper we report the results of both new theoretical calculations and new shock-compression experiments on iodine. We have calculated the 0-K and finite-temperature isotherms for fcc monatomic iodine, and from these determined the Hugoniot (the shock-compression P - V curve). We have, in addition, estimated the Hugoniot for the molecular phase of iodine. The computed monatomic Hugoniot is in very good agreement with the Alder and Christian measurements from about 30 to 70 GPa; i.e., below the abrupt change in slope

that they report. Above 70 GPa our calculations continue smoothly and do not reproduce that anomaly, and are, in fact, not even in qualitative agreement with their measurements. Troubled by the disagreement and suspecting a systematic error in their procedure at the higher pressures, we have repeated the shock experiments above 70 GPa. These new results extend up to about 180 GPa. They show no evidence of the discontinuity observed by Alder and Christian and also constitute a smooth continuation of their measurements below 70 GPa. Our calculated Hugoniot is in good agreement with the new data up to about 140 GPa, above which our neglect of liquid corrections may no longer be adequate.

We judge from this work that there is no sharp break in the Hugoniot in the vicinity of 70 GPa. However, we do not necessarily conclude from this fact that insulating molecular iodine transforms directly into a monatomic phase in the range of 4–17 GPa. This remains a strong possibility, although it would entail a gradual and continuous rearrangement of the iodine molecules prior to the transition in such a way that it would not be first order. A definitive conclusion will require a high-pressure determination of structure above 4 GPa, and we encourage such an experiment, which is within the limits of current experimental capability.¹³ The rather good agreement of our calculations with the shock data over the range of 30–140 GPa does suggest at least that a monatomic phase is a good approximation to the true state.

The organization of the paper is as follows. In Sec. II we describe the shock-compression measurements carried out on the Lawrence Livermore Laboratory two-stage light-gas gun. In Sec. III we report our theoretical isotherm and Hugoniot calculations. The electronic energy and pressure are determined by an approximation to the finite-temperature self-consistent-augmented-plane-wave- $X\alpha$ (SC-APW- $X\alpha$) method. The nuclear vibrational contributions to the energy and pressure are obtained by means of a Grüneisen model. Electron-phonon coupling, anharmonic lattice vibrational effects, and liquid corrections are neglected. Finally, we summarize the work in Sec. IV.

II. EXPERIMENTAL

Before describing our new shock-compression measurements of the iodine Hugoniot, we briefly review some of the parameters involved in such experiments. These matters are covered at length in several review papers.^{14,15}

Shock waves of the type concerned in this work

are characterized by two parameters: the velocity of the shock front in the material (shock velocity U_s) and the velocity imparted to the material behind the front (particle velocity U_p). The thermodynamic properties (P, V, E) of the compressed substance behind the shock front are determined from those of the initial state (P_0, V_0, E_0) and from the shock-wave parameters, according to the Rankine-Hugoniot relations

$$P - P_0 = \rho_0 U_s U_p, \quad (1)$$

$$V = V_0(1 - U_p/U_s), \quad (2)$$

$$E - E_0 = \frac{1}{2}(P + P_0)(V_0 - V). \quad (3)$$

The quantity ρ_0 is the initial density.

The pressure-volume relationship determined from shock-compression experiments (the Hugoniot) is the locus of final states (P, V) obtained by compressing a given initial state (P_0, V_0) with shock waves of different strengths. The shock process is adiabatic, but not reversible. Thus, while the Hugoniot is initially tangent to an isentropic compression curve, its pressure rises more steeply with decreasing volume. This occurs because the amount of irreversible heating increases with shock strength.

Shock data are often more conveniently viewed in a U_s -vs- U_p plot. It is an empirical fact that the relationship between these velocities is fairly linear within a given phase. Changes of slope and other structure are taken to be symptomatic of phase transitions.

A. Experimental procedure and sample preparation

In the present experiments, the shock pressure was obtained by impacting a high-velocity tantalum plate onto a tantalum cover plate of the sample container with subsequent transmission of the shock into the iodine sample. The impactor plate was accelerated by the Lawrence Livermore Laboratory (LLL) two-stage gas gun. Shock velocity through the iodine sample was obtained from the sample thickness measurement, and the time interval between electrical shock-pin closures set flush with the faces of the cylindrical sample and recorded on fast writing oscilloscopes. The particle velocity was obtained indirectly from the tantalum impactor velocity U and the known Hugoniot for tantalum, using the so-called impedance-matching analysis method.^{16,17} The impactor velocity was measured between muzzle and target over a distance of about 15 cm. An x-ray photograph was taken of the projectile in flight. The time interval from x-ray flash to shock-pin closures in the target was recorded on a nanosecond counter, and the distance to target measured from

the x-ray photograph.

Because iodine has a very high vapor pressure at normal temperatures and its vapor is highly corrosive and toxic, it was not feasible to allow the impactor to strike directly onto the unexposed iodine sample surface. Also, the experimental chamber in the two-stage gas gun is required to be evacuated at shot time, and it was found that a significant amount of the sample vaporized during the required exposure to the vacuum. Therefore, a cover plate was used to seal the sample chamber. This plate constituted an intermediate material between impactor and iodine sample surface.

A 1-mm-thick tantalum plate was chosen as the intermediate material to match the tantalum impactor plate (2-mm thickness). Tantalum has a high density, $\rho = 16.67 \text{ g/cm}^3$, therefore a high-shock impedance, and is thus capable of imparting high-shock pressures into the iodine. It is also readily available in 99.9% purity. Tantalum has been used as a standard material at LLL and considerable shock data have been collected. The shock-Hugoniot data for tantalum were required in the analysis of the experiments.¹⁸

The iodine samples were pressed into 19.05-mm-diam cylindrical samples from 99.999% pure iodine crystals. A pressure of about 30 MPa was applied to each sample and resulted in a sample density of $4.92 \pm 0.01 \text{ g/cm}^3$ at 26 °C. At this same temperature, the x-ray density of single crystal iodine is 4.94 g/cm^3 .¹⁹ All pressing and assembly operations were done in a plastic bag filled with dry argon gas to reduce the iodine reaction with water vapor in the air and the resulting corrosive effects on metal parts.

Each cylindrical iodine sample was placed within a cavity of the same size that had been machined into an aluminum plate. This sample container also served for mounting and locating the shock-pin indicators. Six pins were equally spaced around the cavity flush with the side of the iodine sample facing the impactor. Seven more pins were arranged near the center of the cavity and flush with the second iodine surface. One center pin was surrounded by the other six, which were set on a 6.5-mm-diam circle. The signal produced by the electrical shorting of each pin upon arrival of the shock was recorded; and from the resulting time interval, the shock-wave velocity through the sample was calculated. The 1-mm tantalum cover plate was held in place against the iodine surface and the outer six pins by a retainer ring and gasket seal.

Several precautions were taken to minimize the possibility of introducing rarefaction-wave interference²⁰ in these measurements. First, the thickness dimensions of the tantalum impactor

plate, cover plate, and iodine sample were determined at each experimental pressure such that a rarefaction wave could not overtake the shock front during the shock-wave velocity measurements. It was, in fact, possible to take the impactor and cover plate thicknesses to be the same for all shots. Lateral rarefactions initiated from the edge of the impactor and sample sides were considered carefully in setting the diameter and thickness, and the shock-detector pins were set well away from the edges. As a test for experimental variation resulting from geometry, shock measurements were made on two sample thicknesses at the same pressure.

B. Data analysis

The six shock detector pins set flush with the impact side of the sample were sufficient to determine the tilt angle of the flat impactor plate. The six pins set on the second surface were aligned with the first so that the time interval measured by two pairs of pins on each of three diagonals of the array could be compared, thus giving an indication of any possible impact plate distortion. Comparison of the average shock arrival time indicated by the six top pins and the center pin in the array gave further information on plate distortion. Although the plate tilt across the impact pins was as much as 50 nsec, the indicated distortion²¹ was never more than 3 or 4 nsec.

The shock-impedance method of shock-wave analysis is well documented^{16,17} and will not be discussed in detail. The shock pressure produced by the symmetric impact of the tantalum impactor on the tantalum cover plate can be obtained from the measured impactor velocity and the known Hugoniot relation for tantalum. For a symmetric impact $U_p = \frac{1}{2}U$, and for tantalum¹⁸

$$U_s = 3.414 + 1.201U_p. \quad (4)$$

The dynamic impedance $\rho_0 U_s$ of iodine is considerably smaller than tantalum, so the transmitted pressure into the iodine samples is determined by the adiabatic pressure release in the shocked tantalum cover plate. Therefore, the tantalum release adiabatic must be calculated for each experimental pressure. The Hugoniot itself is a good approximation to the adiabat at low pressures and temperatures, but at the extreme shock pressures and temperatures attained in these experiments the possibility of significant corrections existed. However, computer calculations of the tantalum adiabat at the highest pressures attained resulted in a correction to U_p of iodine of less than 0.2%.²²

TABLE I. Experimental results for the iodine shock Hugoniot. The sample thickness (T), impactor velocity (U), particle velocity (U_p), shock velocity (U_s), pressure (P), and relative volume (V/V_0) are shown.

(mm) T	(km/sec) U	(km/sec) U_p	(km/sec) U_s	(GPa) P	V/V_0
4.0	$3.66 \pm 0.5\%$	$2.69 \pm 1\%$	$5.56 \pm 1\%$	$73.8 \pm 2.5\%$	$0.516 \pm 2\%$
5.0	4.60	3.33	6.43	105.3	0.482
4.0	4.65	3.36	6.51	107.6	0.484
3.5	5.53	3.96	7.16	139.5	0.447
3.5	5.40	3.86	7.15	135.8	0.460
3.5	6.58	4.67	7.87	180.8	0.407
3.0	6.64	4.73	7.79	179.9	0.393

C. Results and discussion

Our results are presented in Table I and in Figs. 1 and 2. The figures also show the earlier Alder and Christian measurements as well as our theoretical calculations described in the next section. Note in Fig. 1 that the new data constitute a

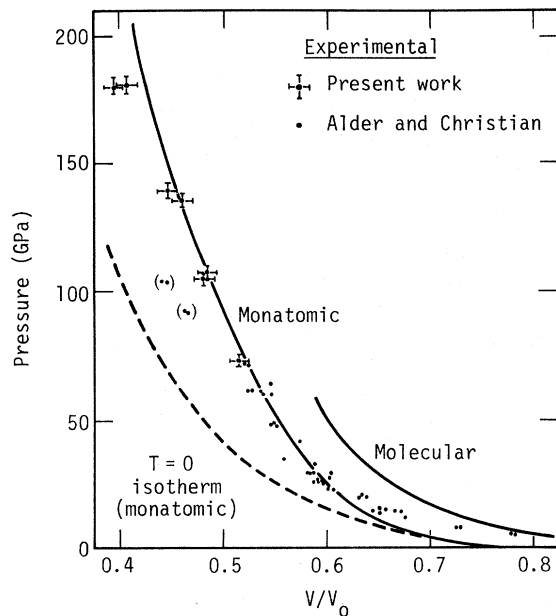


FIG. 1. Iodine Hugoniot. The calculated Hugoniot of monatomic iodine and an estimate of the Hugoniot for the molecular phase are compared to both the new shock-wave data and to the earlier data of Alder and Christian. The anomalous high-pressure points reported by Alder and Christian are enclosed in parentheses. The data appear to shift from one to the other of the computed Hugoniot in the range of 5 to 30 GPa, suggestive of a gradual transition from molecular to the monatomic phase. The computed monatomic Hugoniot is in good agreement with the data from about 30 to 140 GPa. For convenience the calculated 0-K isotherm of fcc monatomic iodine is shown.

smooth continuation of the Alder and Christian results below 70 GPa, but are in conflict with their results above this pressure (the four data points enclosed in parentheses).

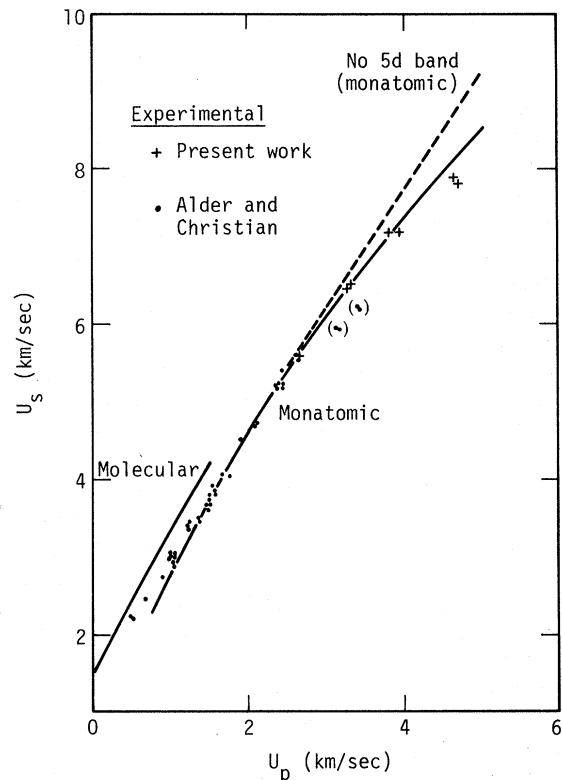


FIG. 2. Shock velocity (U_s) vs particle velocity (U_p) for shock-compressed iodine. This figure shows U_s - U_p plots of the same data and theoretical Hugoniot results as presented in Fig. 1. Gradual curvature is apparent in both the data and the computed monatomic curve for $U_p > 2.4$ km/sec. This feature is interpreted as resulting from thermal excitations into the previously empty 5d band. With the 5d band arbitrarily removed from the calculations, the computed monatomic curve becomes that given by the dashed line.

We suspect a systematic error in the Alder and Christian data above 70 GPa. In these early (1960) experiments shock waves were generated by impacting explosively driven monel or brass flyer plates onto aluminum base plates, to the opposite side of which were affixed the iodine samples. Because of limitations inherent in these explosive techniques, it was necessary to use rather thin flyer plates (monel, 1.59 mm) to achieve sufficiently high flyer-plate velocities for the four high pressure points. Unfortunately, this enhances the possibility of the rarefaction wave²⁰ reflected from the back side of the thin flyer plates overtaking the shock wave before its complete transversal of the iodine sample. Their relatively thick (4.76-mm) aluminum base plate compounded this problem, since this increased the transit time of the shock, thus permitting more time for the faster secondary wave to overtake it. Using known values or reasonable estimates for the shock, particle, and rarefaction velocities in monel, aluminum, and iodine, we estimate that catchup of the rarefaction wave did indeed occur before the shock had transversed half way through the 6.35-mm iodine samples. The effect of such a catchup is to relax the shock front and result in a measured shock velocity (and thus pressure) that is too small. All of the data points below 70 GPa were obtained with flyer plates of 3.0-mm thickness or more and should not have been affected by this problem.

The present experiments were designed carefully to avoid rarefaction-wave interference, as was noted earlier. Use of the two-stage gas gun permitted acceleration of somewhat thicker impactors or flyer plates than could have been achieved with explosive techniques. Also, the thickness of the cover plate and sample combined was taken to be fairly small. As a test, the measurements at 100 and 180 GPa were both repeated with different sample thickness. There was no indication of a significant effect on the data resulting from sample thickness as would be expected if rarefaction-wave interference were present.

Although the six high-pressure data points lie considerably nearer a straight line extrapolation of the lower-pressure U_s -vs- U_p data (Fig. 2), they show a definite deviation from linearity. The physical interpretation of this feature will be deferred to Sec. III.

III. THEORETICAL

One of the unique characteristics of shock-compression experiments is the extremely high experimental temperature that is attained for the short time during which the pressure and density are deter-

mined. In the present case of iodine, the calculated temperature along the Hugoniot at 70 GPa was 11 000 K; and at 140 GPa, 22 000 K. To compare shock-wave measurements with theory, the commonly adopted procedure is the one first outlined by Rice *et al.*,¹⁴ in which the Hugoniot is reduced to a 0-K isotherm using a Grüneisen model. This model specifies the temperature dependence of the energy and pressure by

$$E(V, T) = E_0(V) + 3k_B T, \quad (5a)$$

$$P(V, T) = P_0(V) + 3\gamma k_B T/V, \quad (5b)$$

where $E_0(V)$ and $P_0(V)$ are the corresponding 0-K quantities. The Grüneisen parameter γ is a function of volume only, not of temperature. It is either assumed to have some simple functional form or computed using the thermodynamic definition $\gamma = V(\partial P/\partial E)_V$. Equations (5a) and (5b) presume that the lattice vibrations are harmonic insofar as temperature effects are concerned, and they neglect electronic excitations. These points are often not appreciated by solid-state theorists when comparing their calculated isotherms to high-temperature experiments that have been reduced to 0 K.

In the present work we have undertaken a direct calculation of the Hugoniot for monatomic iodine. We have improved on the techniques just described by explicitly including the effects of electronic excitations. The nuclear motion, however, is still treated with the Grüneisen model.

In outlining our calculations in more detail, it is instructive to note what approximations are made in regard to a fully rigorous finite-temperature theory of metals. As before it is convenient to express the total energy and pressure in terms of ground-state and thermal contributions

$$E(V, T) = E_0(V) + \Delta E(V, T), \quad (6a)$$

$$P(V, T) = P_0(V) + \Delta P(V, T). \quad (6b)$$

We will neglect electron-phonon interactions, both in the ground state, and at finite temperatures. Since the nuclear zero-point energy and pressure are rather small on the scale of interest in this work, the ground-state energy and pressure may then be computed by self-consistent electron-band theory, presuming a rigid lattice of nuclei. Accordingly, we have used the SC-APW- $X\alpha$ method to compute $E_0(V)$ and $P_0(V)$, taking the nuclei in an fcc lattice.

The neglect of electron-phonon interactions at finite temperatures permits separation of the thermal energy and pressure into uncoupled contributions from the electronic excitations and from the nuclear vibrational excitations

$$E(V, T) = E_0(V) + \Delta E_e(V, T) + \Delta E_n(V, T), \quad (7a)$$

$$P(V, T) = P_0(V) + \Delta P_e(V, T) + \Delta P_n(V, T). \quad (7b)$$

In this approximation the contributions from electronic and nuclear vibrational excitations are computed separately, assuming the other subsystem to be in its ground state. We might thus obtain $\Delta E_e(V, T)$ and $\Delta P_e(V, T)$ by performing finite-temperature SC-APW- $X\alpha$ calculations, again presuming a rigid lattice. However, we have shown in the previous paper²³ that the results of such calculations can be very well approximated by a simple model based only on ground-state electronic properties. Accordingly, in this work we shall take

$$\Delta E_e(V, T) = \sum_i \epsilon_i(V) [n_i(T) - n_i(0)], \quad (8a)$$

$$\Delta P_e(V, T) = - \sum_i \frac{d\epsilon_i(V)}{dV} [n_i(T) - n_i(0)], \quad (8b)$$

where $\epsilon_i(V)$ are the *ground-state* eigenvalues obtained from the same SC-APW- $X\alpha$ calculations used to generate $E_0(V)$ and $P_0(V)$; and $n_i(T)$ is the Fermi-Dirac distribution function

$$n_i(T) = \{\exp[\beta(\epsilon_i - \mu)] + 1\}^{-1}. \quad (9)$$

The chemical potential μ is determined by the sum over n_i .

We make the Grüneisen approximation for the nuclear thermal properties

$$\Delta E_n(V, T) = 3k_B T, \quad (10a)$$

$$\Delta P_n(V, T) = 3\gamma k_B T/V, \quad (10b)$$

and compute the Grüneisen parameter from the 0-K isotherm $P_0(V)$ by means of the Dugdale-MacDonald formulation¹⁴

$$\gamma(V) = - \frac{V}{2} \frac{\partial^2 [P_0(V) V^{2/3}] / \partial V^2}{\partial [P_0(V) V^{2/3}] / \partial V} - \frac{1}{3}. \quad (11)$$

As already noted, this approximation presumes the nuclear vibrations to be harmonic.

Our calculations are for an fcc solid phase of monatomic iodine, and are therefore applicable at the higher temperatures only insofar as liquid disorder corrections are small. We shall argue that this is the case over much of the density-temperature range covered by the experimental data.

Once the finite-temperature energy and pressure are known, the final step is to solve the Rankine-Hugoniot relation, Eq. (3), for the Hugoniot of monatomic iodine. This relation is applicable despite the fact that the initial state is diatomic molecular iodine. Furthermore, it will not be necessary to actually determine the total energy E_0 of this initial state. Equation (3) depends only

on energy differences, and the cohesive energy of normal-density diatomic molecular iodine is known from experiment. We may therefore shift the problem instead to a determination of the cohesive energy of the monatomic phase, which is within the scope of our calculations.

A. Ground-state calculations

Our prescription for computing the Hugoniot of monatomic iodine requires information from ground-state self-consistent electron-band structure calculations: energy, pressure, one-electron eigenvalues, and the nuclear Grüneisen parameter. In addition, a comparable calculation for the isolated iodine atom is needed to obtain the cohesive energy.

The ground-state calculations were performed using the SC-APW- $X\alpha$ method, which has been discussed in the previous paper²³ and in several review articles.^{24,25} The value of α for the $X\alpha$ exchange-correlation approximation was taken to be 0.7001, so that the total energy of the isolated iodine atom obtained using the same $X\alpha$ approximation would be equal to the total Hartree-Fock energy.²⁶ In the SC-APW- $X\alpha$ calculations, all electrons were included and treated self-consistently with the localized innercore electrons treated in a self-consistent atomic fashion. When wave functions of core electrons treated in this atomic fashion were found to extend to the edge of the muffin-tin sphere, the calculations were repeated and these energy levels were computed by the band method. Over the range of compressions investigated, we found it necessary to treat the $4d$ states (and the $4p$ states as a precaution) in the band mode in addition to the $5s$ - and $5p$ -valence states. The $4p$ and $4d$ bands were calculated with the equivalent of 32 points in the full Brillouin zone; the $5s$ and $5p$ bands, with 256 points. The use of a small number of points for the filled narrow inner bands is a good approximation as has been verified by ourselves and others.²⁷ We judged that 256 points for the $5s$ and $5p$ bands were adequate when a calculation at one volume with 2048 points yielded a total energy and pressure different by only a few millirydbergs and a few kilobars, respectively. The radial mesh was of the Herman-Skillman²⁸ doubling form with 344 points out to the muffin-tin sphere radius. Sums over angular momentum were truncated after 13 values. Running time on the CDC-7600 was a bit under 2 min/iteration, and generally 10 iterations were required for convergence of the total energy and pressure to about ± 0.0005 Ry and ± 0.5 kbar, respectively.

Our results for the ground-state energy and

TABLE II. Theoretical results for the ground-state energy and pressure of fcc monatomic iodine. The energy (E) and pressure (P) were obtained from SC-APW- $X\alpha$ calculations. Estimates of the non-muffin-tin corrections to these quantities are given by E_{nmf} and P_{nmf} , respectively.

V/V_0	E (Ry)	P (GPa)	E_{nmf} (Ry)	P_{nmf} (GPa)
0.40	-13 835.8453	109.65	-0.0181	-3.42
0.44	-13 835.9168	75.54	-0.0156	-2.84
0.51	-13 835.9936	39.98	-0.0123	-2.08
0.55	-13 836.0203	28.04	-0.0108	-1.75
0.65	-13 836.0555	10.39	-0.0081	-1.17
0.75	-13 836.0673	2.20	-0.0061	-0.81

pressure of fcc monatomic iodine are presented in Table II. Volume is specified by the ratio $v = V/V_0$, where V_0 is the volume *per atom* of normal-density diatomic molecular iodine at 299 K ($V_0 = 287.703 \text{ bohr}^3 = 25.674 \text{ cm}^3/\text{mole I}$).¹⁹ The second and third columns of Table II give the total energy per atom and pressure as obtained from the SC-APW- $X\alpha$ calculations. These pressures were computed by means of the virial theorem. Since monatomic iodine with five p -type valence electrons is a rather unusual metal, we thought it prudent to test the accuracy of the muffin-tin approximation used in the SC-APW- $X\alpha$ calculations. Our estimates of the non-muffin-tin corrections to the energy and pressure are given in the last two columns of Table II and are described in the Appendix. Although these corrections are rather small, we have included them in the Hugoniot calculations.

The SC-APW- $X\alpha$ energies and pressures in the second and third columns of Table II could be fit with the functional form $a \exp(-bV^{1/3}) + c - d/V^2$ and its negative derivative to within an rms deviation of $\pm 0.0004 \text{ Ry}$ and $\pm 0.27 \text{ GPa}$, respectively. This satisfaction of the virial theorem is a strong indication that self-consistency was indeed achieved in the SC-APW- $X\alpha$ calculations. With the parameters slightly changed to reproduce the results including non-muffin-tin corrections, the same analytic form was used to compute the nuclear Grüneisen parameter according to Eq. (11).

The electron-band structure in the $[100]$ direction is shown in Fig. 3 at three volumes. The band energies are measured relative to the constant potential outside of the muffin-tin spheres. Included in the figure are the $5s$, $5p$, and part of the $5d$ - $6s$ bands. The $4p$ and $4d$ bands were of course extremely narrow and are not shown. For purposes of later discussion, it is noted that the gap between the Fermi energy (ϵ_F) and the bottom of the

$5d$ band (ϵ_{X_1}) is decreasing rather rapidly with compression. As to the volume dependence of the eigenvalues, we were in all cases able to obtain excellent fits using the functional form $a + bV + cV^{-d}$. These analytic fits were used to obtain the volume derivatives of the eigenvalues for Eq. (8b).

The usual procedure for calculating cohesive energies is to subtract the total computed solid energy per atom from the total computed atom energy, using the same local exchange-correlation approximation, i.e., the same α , in both sets of calculations. This procedure can be expected to be reliable if the errors made in the exchange-correlation approximate calculations of the total energy originate well inside the atom cores, and α is thus a volume-independent constant. This appears to be the case as such cohesive energy calculations generally agree with experiment to within $\pm 20\%$, which is rather good agreement.²⁹

We have obtained the energy of the isolated iodine atom as $-13 835.973 \text{ Ry}$, using the same α , by running the SC-APW- $X\alpha$ code in a purely atomic mode for a very large lattice constant. It has been emphasized recently that for cohesive energy calculations involving atoms with unfilled shells, one should include spin-polarization effects in treating the isolated atom.³⁰ We have not done so, but can estimate a lowering of the atom energy over our non-spin-polarized calculation by

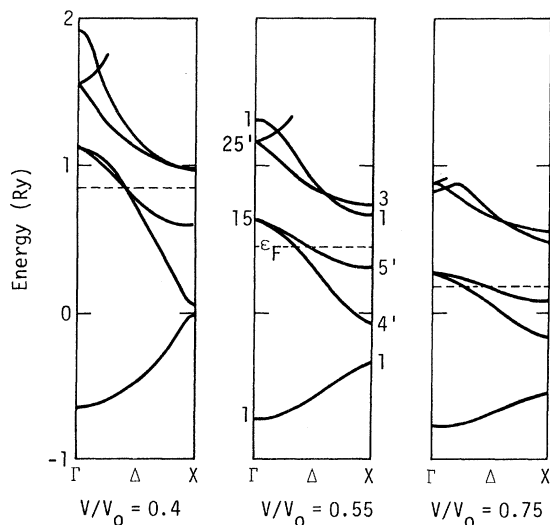


FIG. 3. Band structure of fcc monatomic iodine. The 0-K band structure is given in the $[100]$ direction at three volumes. The $5s$, $5p$, and part of the $5d$ - $6s$ bands are shown. The Fermi energy is indicated at each volume by the dashed line. Note that the gap between the bottom of the $5d$ band (X_1 state) and the Fermi energy is decreasing fairly rapidly with compression.

about 0.02 Ry.³¹ Taking this into account and the solid energies in Table II, we estimate the zero-pressure cohesive energy of fcc monatomic iodine to be about 0.08 Ry/atom. This may be compared to the experimental cohesive energy of normal-density diatomic molecular iodine, which is 0.081 Ry/atom relative to isolated atoms.³² Since the stable structure at one atmosphere is the molecular phase, the cohesive energy of the monatomic phase must be less. Presuming our estimate to be good to within 20% or so, we anticipate that the zero-pressure cohesive energy of the monatomic phase is 0.06 to 0.08 Ry/atom.

We may obtain a more precise value of the energy difference between the zero-pressure monatomic and molecular phases contingent upon an assumption about the transition pressure. An isotherm extending up to 15 GPa has been obtained from analysis of the Hugoniot data.¹¹ This region is below the complicated thermal electronic effects described in Sec. III B, so the result should be reliable. When this molecular isotherm is compared with our results in Table II, it is seen that the two curves appear to be approaching a point of tangency somewhere just beyond 15 GPa. If there were a transition in this region, it would be a weak first-order, or conceivably a higher-order transition as would be consistent with static-resistivity measurements. At the transition the Gibbs free energies of the two phases at 0 K would have to be equal. By integrating under the P - V curve of each phase from $P=0$ to this transition, one can determine the initial energy difference between the two phases at zero pressure. This leads to the energy of the molecular phase being 0.01 Ry lower. This figure is within the theoretical uncertainties discussed in the preceding paragraph. We will use this energy difference of 0.01 Ry to set the energy E_0 for the initial state in the Hugoniot calculations in Sec. III B.

We have tested the sensitivity of both pressure and cohesive energy to the choice of α at a relative volume of $v=0.51$. For $\alpha = \frac{2}{3}$ the pressure was 4.8 GPa larger than our tabulated value (40.0 GPa) obtained with $\alpha = 0.7001$, and for $\alpha = 0.7335$ it was smaller by 4.8 GPa. The cohesive energy variation was less linear, decreasing by 0.024 Ry from $\alpha = 0.7001$ to $\frac{2}{3}$ and increasing by 0.019 Ry from $\alpha = 0.7001$ to 0.7335. It is emphasized that these tests represent very large changes in the parameter α . The two most commonly used prescriptions for choosing α (α_{HF} and α_{VT} , see Ref. 33) generally yield values of this parameter that differ by less than 0.001. As we have used the former prescription, it is clear that the quantities calculated in this section will only be negligibly changed by use of the latter.

B. Hugoniot calculations

Hugoniot calculations were carried out for monatomic iodine. The initial E_0 , P_0 , and V_0 were taken as those of molecular iodine at room temperature and 1 atm of pressure. We took E_0 to be 0.01 Ry/atom lower than the zero-pressure (≈ 1 -atm) energy of the monatomic phase as discussed earlier. Using the energies $E(V, T)$ and pressures $P(V, T)$ computed according to Eqs. (7a) and (7b), the Hugoniot was determined by finding the temperature and pressure for which the Rankine-Hugoniot relation, Eq. (3), was satisfied at each volume.

In evaluating the thermal electronic energy and pressure according to Eqs. (8a) and (8b), we included the 5s and 5p states and the 5d-6s states up to the highest energies for which the band structure is plotted in Fig. 3. To test for possible problems that might arise from this cutoff, we also performed the Hugoniot calculations using a free electron density of states (with an appropriate effective mass) for the 5d-6s band and extended them to arbitrarily high energies. We obtained essentially the same results. It is worth noting in regard to these matters that over the range of densities and temperatures encountered along the Hugoniot in our calculations, the chemical potential is never more than 0.03 Ry higher than the Fermi energy. The chemical potential first increases with temperature because of the decreasing density of states at the Fermi energy. As the 5d band becomes thermally accessible, the trend reverses and the chemical potential begins to decrease relative to the Fermi energy.

Figure 1 compares the Hugoniot calculated for monatomic iodine with experimental data. The corresponding 0-K isotherm (dashed line) is also given so that the amount of thermal pressure may be seen as the difference between the two curves. An estimate of the molecular-phase Hugoniot has been obtained using an exponential-6 potential assuming spherical iodine molecules on an fcc lattice.³⁴ The parameters were taken to fit normal-density experimental data. The agreement between molecular calculations and data is clearly best in the limit of low pressures and becomes successively poorer at the higher pressure where the monatomic calculations are in better agreement. The apparent shifting with compression of the agreement between the data and the two calculated Hugoniots is at least suggestive of a gradual transition from the molecular to a monatomic phase. This feature is also evident in a $U_s - U_p$ presentation of the results shown in Fig. 2.

Our choice of E_0 has in effect optimized agreement with the data at low pressures. Our theo-

retical uncertainty in this parameter is about ± 0.01 Ry, and a change in E_0 by this amount would alter the Hugoniot at $v=0.6$ by 3.5 GPa. It should be noted that 3.5 GPa is still within the experimental scatter at this volume. The higher pressure points are much less sensitive to this choice. Nevertheless, our choice of E_0 is consistent with the general degree of reliability of SC-APW- $X\alpha$ cohesive energies, with a very weak first-order transition to the monatomic phase, and with the onset of metallic conductivity under static compression of about the right experimental pressure.

Aside from the choice of E_0 , the major uncertainty in calculating the Hugoniot is the choice of the nuclear Grüneisen parameter. The Dugdale-MacDonald formulation, which we have used, is generally preferred as it is known to give better agreement with experiment at normal density. The nuclear contribution is everywhere 80% or more of the total thermal pressure, and alternate expressions for γ give values both larger and smaller by about 5% than those we have used.³⁵ With the larger values, the Hugoniot pressure would be increased by about 10, 5, and 1 GPa at $v=0.45$, 0.55, and 0.65, respectively, or still within reasonably close agreement of the data.

Using the Lindemann law in conjunction with sound velocities calculated from the 0-K isotherm, we estimated melting along the Hugoniot to occur in the vicinity of $v=0.61$ at a temperature of about 2500 K. Consequently, much of the data in Fig. 1 corresponds to a liquid phase of iodine. Nevertheless, we do not expect liquid corrections to be large until the highest compressions in the figure. Our experience with shock-compressed argon, which has a relatively high volume change on melting (15% at normal density), has shown that the observed shock Hugoniot is insensitive to the melting line. In addition, argon Hugoniots calculated with liquid perturbation theory and the solid-like Lennard-Jones-Devonshire cell model both predicted Hugoniots within experimental error for the same pair potential.³⁶ The electronic contribution to the thermal energy and pressure depends only on gross features of the electronic density of states, which may be expected to be preserved in going from solid to liquid in view of the marked similarity in liquid and solid metal electrical conductivities.³⁷ In addition, scaling-law arguments for monatomic metals³⁸ suggest that Grüneisen models for the solid may be extended with reasonable accuracy up to temperatures perhaps a factor of four larger than the melting temperature appropriate to the given density. Such a temperature ratio exists at $v=0.45$ in Fig. 1. A model calculation based on these scaling-

law arguments indicates that the liquid corrections are of the same sign and same order of magnitude as the discrepancy between theory and experiment apparent in the upper part of the Hugoniots in Fig. 1.

C. Effect of electronic excitation on Hugoniot

A particularly noteworthy feature of both the data and theoretical results is a significant softening of the Hugoniot at the higher temperatures and pressures. This softening is best viewed in the shock-particle velocity plane given in Fig. 2 and is represented by the gradual curvature for the U_p above 2.4 km/sec. A similar effect has been observed in shock-compressed xenon and was interpreted as resulting from thermal excitations into the $5d$ band.³⁹ This same mechanism appears to be operating in iodine. As seen in Fig. 4, even at the highest density a gap exists between the bottom of the $5d$ band and the Fermi level (solid line, $\epsilon_{x_1} - \epsilon_F$). There are no electrons in $5d$ states at zero temperature. In shock compression, however, the increasing temperature along the Hugoniot (solid line, $k_B T_h$) eventually becomes comparable to the gap and results in thermal excitations into the $5d$ band. The number of electrons per atom that occupy such states is given by the dashed curve. If the iodine Hugoniot calculation is repeated using only the $5p$ band and excluding the $5d$ and all higher bands, one gets the dashed curve in Fig. 2, which shows much less curvature and corresponds to a stiffer Hugoniot. Clearly then, a proper characterization of the Hugoniot requires inclusion of the correct electronic structure.

The important physical feature in the softening of the Hugoniot is the decreasing $5p$ to $5d$ band

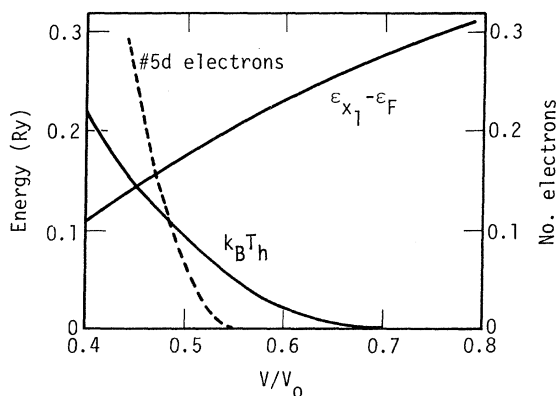


FIG. 4. Occupation of the $5d$ band along the Hugoniot. The gap between the $5d$ band and the Fermi energy ($\epsilon_{x_1} - \epsilon_F$) and the temperature along the Hugoniot ($k_B T_h$) are plotted as a function of relative volume. When the temperature becomes comparable to the gap, electrons are excited into the $5d$ band. The number of electrons per atom which are excited into this band is given by the dashed curve (right-hand scale).

gap. An excitation from the $5p$ to the $5d$ band requires a relatively large energy. However, since the $5p$ to $5d$ gap (ϵ_F to ϵ_{x_1}) is narrowing with compression, such an excitation leads to a positive $d(\epsilon_{x_1} - \epsilon_F)/dV$ and therefore to a negative contribution to the total thermal pressure as given in Eq. (8b). The $5d$ states thus serve as a sink that absorbs energy (without an increase in thermal pressure) that would otherwise have gone into excitation of the electrons to higher kinetic energy states within the $5s$ - $5p$ bands, or into thermal motion of the nuclei—both of which would lead to significant increase in thermal pressure. This energy sink mechanism is in effect turned on when the Hugoniot temperature becomes comparable to the gap. As an illustration of these ideas, we show in Fig. 5 the nuclear and electronic Grüneisen parameters along the Hugoniot. The electronic parameter γ_e is defined simply as $V\Delta P_e/\Delta E_e$. The dashed line (no $5d$ band) accounts for only excitations within the $5s$ - $5p$ bands and is seen to be comparable to the Dugdale-MacDonald nuclear gamma. However, with the inclusion of $5d$ states, γ_e is reduced by a factor of 2 at the higher compression.

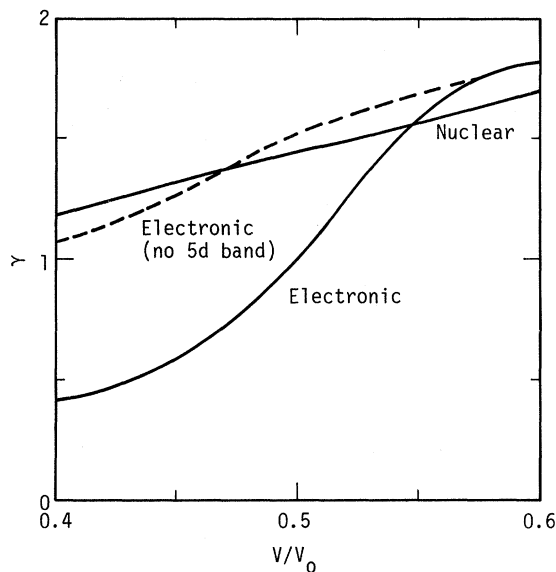


FIG. 5. Grüneisen γ 's along the Hugoniot. The nuclear γ was obtained from the Dugdale-MacDonald relation and is temperature independent. The electronic γ was taken to be $V\Delta P_e/\Delta E_e$ and evaluated at the temperature along the Hugoniot. The abrupt decrease in the electronic γ for relative volumes less than $V/V_0 = 0.55$ is due to the onset of thermal excitations into the $5d$ band, as may be seen by comparison to the dashed curve where the $5d$ band was arbitrarily removed from the Hugoniot calculations. This may be understood by the fact that a $5d$ excitation absorbs a relatively large energy, but because the $5p$ to $5d$ band gap is decreasing with compression, results in only a small change in pressure.

sions. Since an equivalent definition of γ is $\gamma = VdP/C_v dT$, a decrease in γ can be interpreted as meaning the pressure increases less rapidly with temperature, and the resulting Hugoniot must be softer as observed.

Analogous electronic effects resulting from the lowering $5d$ band are observed in the compressed solids of neighboring elements in the Periodic Table, cesium and xenon. Static compression of cesium leads to a shift of electrons from the half-filled $6s$ band to the $5d$ band. The most recent discussions⁴⁰ suggest that this extended transition leads to the unusual softness (low-bulk modulus) of the isotherm below 4.2 GPa; in addition perhaps to the first-order isomorphous-phase transition at this pressure. In the case of xenon (filled $5p$ band) and iodine ($\frac{5}{8}$ filled), the $5d$ band will intersect the Fermi surface at threefold to fourfold compression of the solid. However, the high temperatures that accompany shock compression can thermally excite electrons into the $5d$ band at much lower densities, and thus anticipate $5p$ to $5d$ transitions analogous to the $6s$ to $5d$ transition in cesium. As mentioned above, a softening in the xenon Hugoniot has indeed been observed and identified with this mechanism.³⁹ Similar effects may also occur in the lanthanides and actinides. These effects illustrate the usefulness of the high temperatures generated in shock-wave experiments in providing a unique set of conditions for the study of changes in electronic properties of metals under compression.

IV. SUMMARY

We have reported both experimental measurements and theoretical calculations of the shock Hugoniot of metallic iodine. The data range from 70 to about 180 GPa and constitute a smooth continuation of the earlier lower pressure work of Alder and Christian. We find no evidence for the sharp change of slope around 70 GPa, which they reported and identified with the dissociation of the I_2 molecules. When viewed in a shock-velocity versus particle-velocity plot, however, the combined data shows significant curvature of a gradual nature.

At low pressures or small U_s and U_p 's, our computed monatomic Hugoniot is in poor agreement with experiment, but the one estimated for a molecular phase is in good agreement. The agreement between calculated Hugoniots and the data reverses itself gradually in the range of 5–25 GPa. From about 30 to 140 GPa the computed Hugoniot for the monatomic phase is the one in close agreement with the data. Above this pressure and temperature, liquid disorder corrections

may be too large to be ignored. We conclude that the onset of metallic conductivity in iodine has probably been the result of a gradual structural conversion of the molecular phase to some state comparable to a monatomic arrangement. Our results are not sufficient to deduce whether the lattice is actually monatomic or whether it is an intermediate state, and the actual conversion to monatomic occurs at a somewhat higher pressure. However, in the latter eventuality the results do suggest that any such intermediate conducting state is likely to be close in structure to the monatomic phase, and that band overlap, even in a molecular phase, is connected with some rearrangement to a more closely packed structure.

Although agreement between theory and experiment is less good at the highest pressures, both show significant curvature when viewed in a shock versus particle-velocity plot. At these compressions the temperature is comparable to the gap between the Fermi energy and the bottom of the $5d$ band, leading to large thermal excitations into the previously empty $5d$ band. This band gap is decreasing, and the overall effect of exciting electrons above such a gap is to soften the Hugoniot and introduce the observed curvature into the $U_s - U_p$ plot.

APPENDIX: NON-MUFFIN-TIN CORRECTIONS

An important approximation in the APW or Korringa-Kohn-Rostoker methods is the muffin-tin approximation or assumption of constant charge density and crystal potential in the interstitial regions outside the touching sphere boundaries and spherical symmetry of these quantities within the spheres. The failure of a real metal to satisfy this approximation could compromise the accuracy of the predicted thermodynamic properties. Consequently, numerical estimates of the non-muffin-tin corrections to the total energy were made using the first-order perturbation expression⁴¹

$$E_{\text{nmT}} = \int d^3r [\rho(\vec{r}) - \rho_{\text{MT}}(\vec{r})] [W(\vec{r}) - W_{\text{MT}}(\vec{r})] + \frac{3}{4} C_\alpha \int d^3r [\rho(\vec{r})^{4/3} - \rho_{\text{MT}}(\vec{r})^{4/3}]. \quad (\text{A1})$$

In this expression $\rho(\vec{r})$ is the charge density, $W(\vec{r})$ is just the Coulomb part of the one-electron potential, $C_\alpha = -3\alpha(3/\pi)^{1/3}$, and the subscript MT in each case refers to the muffin-tin approximate quantity.

The integration in Eq. (A1) was confined to the volume between the muffin-tin spheres. The dominant errors will originate there.⁴² Because of the extensive effort required to work with the true self-consistent charge density, we have approximated this quantity within the region of interest by

$$\rho(\vec{r}) = \rho_0 \sum_a \frac{\exp(-\lambda |\vec{r} - \vec{R}_a|)}{|\vec{r} - \vec{R}_a|}. \quad (\text{A2})$$

where the sum is over the neighboring atoms a . This expression is physically motivated by the Thomas-Fermi theory of the atom, and it explicitly incorporates the lattice symmetry. We find that the two parameters ρ_0 and λ may be chosen so that the muffin-tin approximation to Eq. (A2) is in excellent agreement with the correct self-consistent $\rho_{\text{MT}}(r)$ in regard to slope and value just inside the muffin-tin sphere and the constant value outside. Since this information overdetermines the two parameters, there is some reason to feel that Eq. (A2) is a reliable fit to the true charge density in the interstitial region. The Coulomb potential $W(r)$ is trivially obtained from Eq. (A2) by Poisson's equation. Its muffin-tin approximation has a discontinuity at the muffin-tin radius that is within 20% of the correct value. Results of our numerical calculations of Eq. (A1) are presented in the fourth column (E_{nmT}) of Table II. The last column gives the concomitant pressure errors, obtained by differentiation. Although they are small, we have included these corrections in the Hugoniot calculations.

ACKNOWLEDGMENTS

We have benefited in this work from many conversations with our colleagues, R. Grover, J. W. Shaner, M. Van Thiel, D. A. Young, and A. Kusunobov. We also wish to acknowledge the mechanical support of B. R. Morgan, W. D. Barrowman, and M. A. Benapfl, and the electronics support of J. J. Dub.

*Work performed under the auspices of the U. S. Energy Research and Development Administration under Contract No. W-7405-Eng-48.

¹A. S. Balchan and H. G. Drickamer, *J. Chem. Phys.* **34**, 1948 (1961).

²B. M. Riggelman and H. G. Drickamer, *J. Chem. Phys.* **37**, 446 (1962).

³B. M. Riggelman and H. G. Drickamer, *J. Chem. Phys.*

38, 2721 (1963).

⁴R. E. Harris, R. J. Vaisnys, H. Stromberg, and G. Jura, in *Progress in Very High Pressure Research*, edited by F. P. Bundy, W. R. Hibbard, and H. M. Strong (Wiley, New York, 1960), p. 165.

⁵L. F. Vereshchagin, A. A. Sermerchan, N. N. Kuzin, and Yu. A. Sodkov, *Dokl. Akad. Nauk SSSR* **209**, 1311 (1973) [*Sov. Phys.-Dokl.* **18**, 249 (1973)].

- ⁶The pressure scale used by Drickamer and coworkers has been revised cf., H. G. Drickamer, *Rev. Sci. Instrum.* **41**, 1667 (1970).
- ⁷H. L. Suchan, S. Wiederhorn, and H. G. Drickamer, *J. Chem. Phys.* **31**, 355 (1959).
- ⁸S. S. Kabalkina, T. N. Kolobyanina, and L. F. Vereshchagin, *Dokl. Akad. Nauk SSSR* **172**, 313 (1967) [*Sov. Phys.-Dokl.* **12**, 50 (1967)].
- ⁹R. W. Lynch and H. G. Drickamer, *J. Chem. Phys.* **45**, 1020 (1966).
- ¹⁰P. W. Bridgman, *Phys. Rev.* **45**, 893 (1935).
- ¹¹R. Grover, A. S. Kusubov, and H. D. Stromberg, *J. Chem. Phys.* **47**, 4398 (1967).
- ¹²B. J. Alder and R. H. Christian, *Phys. Rev. Lett.* **4**, 450 (1960). Reference 16 contains a recalibration of these data.
- ¹³X-ray techniques can be used in shock as well as static compression, cf., Q. Johnson and A. C. Mitchell, *Phys. Rev. Lett.* **29**, 1369 (1972).
- ¹⁴M. H. Rice, R. G. McQueen, and J. M. Walsh, *Solid State Phys.* **6**, 1 (1958).
- ¹⁵R. G. McQueen, S. P. Marsh, J. W. Taylor, J. N. Fritz, and W. J. Carter, in *High Velocity Impact Phenomena*, edited by R. Kinslow (Academic, New York, 1970), Chap. VII.
- ¹⁶*Compendium of Shock Wave Data*, edited by M. van Thiel (UCRL-50108), June, 1966 (unpublished); Suppl. 1, October 1967, distributed by Natl. Tech. Inf. Service, U. S. Dept. of Commerce, 5285 Port Royal Rd., Springfield, Va. 22151.
- ¹⁷A graphic solution to the impedance-matching analysis is given in J. W. Walsh, M. H. Rice, R. G. McQueen and F. L. Yarger, *Phys. Rev.* **108**, 196 (1957).
- ¹⁸Group Report GMX-6 (LA-4167-MS, May 1, 1969) Los Alamos Sci. Lab., Univ. of Calif., Los Alamos, N. M. 87544 (unpublished).
- ¹⁹R. W. G. Wyckoff, *Crystal Structures* (Interscience, New York, 1963), 2nd ed., Vol. 1, p. 53.
- ²⁰When the impactor (or flyer plate) collides with the cover (or base) plate, not only is a shock wave generated that propagates forward in the cover plate, but another travels backwards in the impactor. This latter shock wave is reflected as a rarefaction or release wave from the back surface of the impactor and returns in the direction of the cover plate. When the rarefaction reaches the cover plate and somewhat later the sample itself, it will travel with a velocity equal to the sound velocity (c) of that already compressed material *plus* the particle velocity (U_p) of that shocked material. By common rule of thumb, $c \sim 1.3U_s$, where U_s is the velocity of the original shock wave in the given material. Thus, in the cover plate and sample, the rarefaction will propagate with a net velocity $c + U_p$, which can be considerably larger than U_s .
- ²¹L. B. Evans, B. L. Hord, A. C. Mitchell, and M. Van Thiel, report (UCRL-51665, 1974) (unpublished), distributed by Natl. Tech. Inf. Service, U. S. Dept. of Commerce, 5285 Port Royal Rd., Springfield, Va. 22151.
- ²²R. G. Grover (private communication).
- ²³A. K. McMahan and M. Ross, preceding paper, *Phys. Rev. B* **15**, 718 (1977).
- ²⁴Detailed descriptions of the APW method and the manner in which it can be made self-consistent are given by T. L. Loucks, in *Augmented Plane Wave Method* (Benjamin, New York, 1967); L. F. Mattheiss, J. H. Wood, and A. C. Switendick, in *Methods in Computational Physics*, edited by B. Alder, S. Fernback, and M. Rotenberg (Academic, New York, 1968), Vol. 8, p. 63.
- ²⁵The $X\alpha$ exchange-correlation approximation is discussed by J. C. Slater, in *Advances in Quantum Chemistry*, edited by P. Lowdin (Academic, New York, 1972), Vol. 6, p. 1.
- ²⁶J. B. Mann, Los Alamos Scientific Laboratory Report No. LA-3690, 1967 (unpublished).
- ²⁷J. B. Conklin, Jr., F. W. Averill, and T. M. Hattox, *J. Phys. Colloque* **3**, C3-213 (1972).
- ²⁸F. Herman and S. Skillman, *Atomic Structure Calculations* (Prentice-Hall, Englewood Cliffs, N. J., 1963).
- ²⁹For specific references to SC-APW- $X\alpha$ calculations of cohesive energies, see Ref. 23.
- ³⁰O. Gunnarsson, B. I. Lundqvist, and J. W. Wilkins, *Phys. Rev. B* **10**, 1319 (1974).
- ³¹J. F. Janak, V. L. Moruzzi, and A. R. Williams, *Phys. Rev. B* **12**, 1257 (1975).
- ³²The cohesive energy relative to separated molecules is given by K. Yamasaki, *J. Phys. Soc. Jpn.* **17**, 1262 (1962). The dissociation energy of the I_2 molecule is given by G. Herzberg, *Molecular Spectra and Molecular Structure* (Van Nostrand, New York, 1950).
- ³³K. Schwarz, *Phys. Rev. B* **5**, 2466 (1972).
- ³⁴The same approach has been used by J. C. Raich and L. C. Bartel, *J. Phys. Chem. Solids* **28**, 1079 (1966). This paper uses simple models for both monatomic and molecular phases of iodine and obtains a transition pressure of 50 GPa at 0 K.
- ³⁵The Slater-Landau formulation (See ref. 14) gives values of γ about 5% larger than those we have used; the free-volume formulation [V. Vashchenko and V. Zubarev, *Fiz. Tverd. Tela* **5**, 886 (1963)], about 5% smaller.
- ³⁶M. Ross, *Phys. Rev. A* **8**, 1466 (1973).
- ³⁷N. W. Ashcroft, *Sci. Am.* **221**, 72 (1969).
- ³⁸R. Grover, *J. Chem. Phys.* **55**, 3435 (1971).
- ³⁹M. Ross, *J. Phys. Chem. Solids* **33**, 1105 (1972).
- ⁴⁰D. McWhan, G. Parisot, and D. Bioch, *J. Phys.* **4**, L69 (1974).
- ⁴¹J. B. Danese, *J. Chem. Phys.* **61**, 3071 (1974).
- ⁴²P. D. DeCicco, Ph.D. thesis (M.I.T., 1965) (unpublished).